

Phenotypic profiling of autophagy using the Opera Phenix high-content screening system.



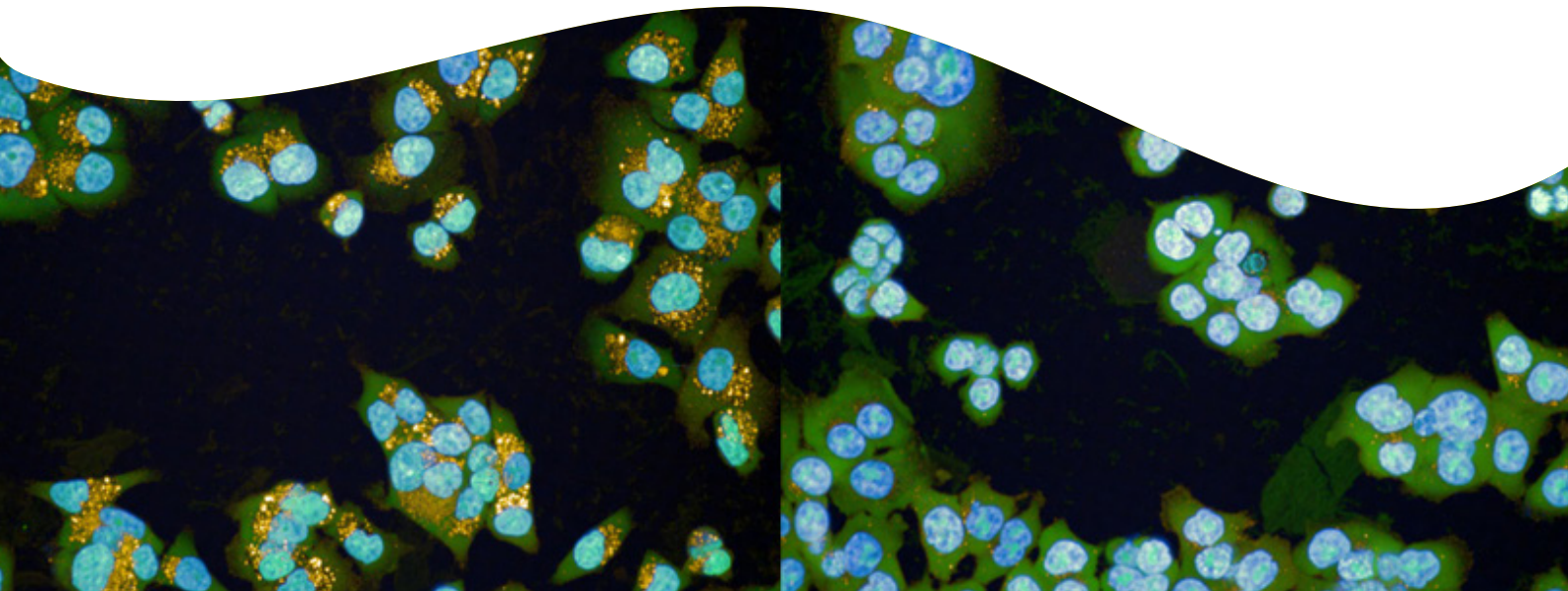
Key features

- Quantification of autophagy using advanced morphology object properties
- Interactive training using PhenoLOGIC™ machine learning technology
- Gain more insights with High Content Profiler™ secondary analysis

Background

Cells constantly sense their environment and their response is a spatio-temporal summation of all signals. To maintain physiological stability, cells need to adjust to environmental changes, a process called homeostasis. One of the most important processes involved in maintaining homeostasis is autophagy, and its significance was recognized by the award of the Nobel Prize for Physiology in 2016 to Yoshinori Ohsumi for the discovery of its underlying mechanisms. Autophagy is the process of degrading cellular components such as lipids, large protein complexes or even whole organelles via the lysosomal route (Figure 1). Autophagy is used to clear the cell and recycle metabolic building blocks. It occurs constitutively but also in response to stress signals. Altered autophagy is found in various pathological conditions, for example, neurodegenerative diseases, cancer and viral and bacterial infections¹. During tumor progression autophagy seems to change from an anti-tumorigenic to a pro-tumorigenic function. Although this is not fully understood, it is believed that autophagy can prevent tumor development by degrading, for example, damaged organelles and protein aggregates. However, especially at later stages of tumor development, enhanced autophagy may help to withstand metabolic and hypoxic stress¹.

For research use only. Not for use in diagnostic procedures.



In this study, we validate a phenotypic image and data analysis workflow provided by Revvity's Harmony® high-content imaging and analysis and High Content Profiler™ software using an autophagy assay as an application example. Alterations in autophagy can easily be visualized using the Opera Phenix™ high-content screening system and characterized by a set of advanced texture and STAR morphology features in the Harmony software. Secondary analysis in High Content Profiler then provides an automated workflow to create extensive data visualizations and cell classification to further the understanding of multiparametric phenotypic screening datasets.

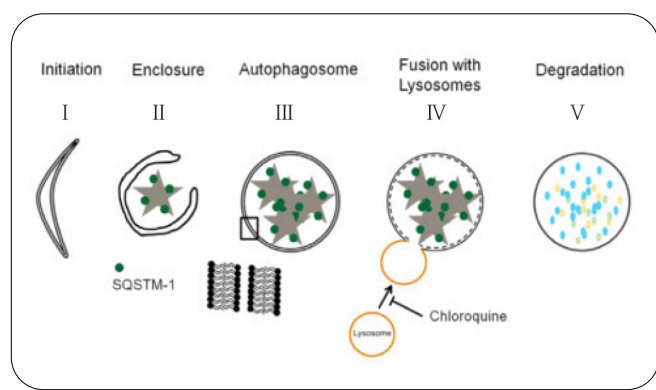


Figure 1: Schematic drawing showing the main steps during autophagosome generation and degradation. The first step is the *de novo* formation of a double membrane structure (I) which then encloses the target or cargo (II) resulting in the formation of a double membrane enclosed vesicle, the so-called autophagosome (III). Autophagosomes then fuse with lysosomes, which subsequently leads to acidification and activation of hydrolases which degrade the inner membrane and the cargo (IV and V). The fusion of lysosomes can be blocked by chloroquine resulting in accumulation of autophagosomes. If normal degradation occurs, the final vesicle contains the degraded cargo from which the metabolic building blocks are recycled (V).

High content assay

HeLa, PANC-1 and HCT116 cells were cultured according to ATCC guidelines (ATCC, Manassas, Virginia). For imaging, 2.5×10^3 HeLa and PANC-1 cells and 5×10^3 HCT 116 cells were seeded into each well of a PhenoPlate 384-well plate (Revvity, Waltham, MA, Product # 6057300). After incubation overnight to allow attachment, cells were treated with chloroquine concentrations (chloroquine diphosphate, Tocris, Abingdon, UK) ranging from $1.6 \mu\text{M}$ - $100 \mu\text{M}$ for 18 hours to enrich autophagosomes (see Figure 1, IV).

Autophagosomes were stained using an anti-human SQSTM-1 antibody (R&D Systems, Inc., Minneapolis, MN Cat# MAB8028) and a Northern Lights 557 conjugated secondary antibody (R&D Systems, Inc., Minneapolis, MN, Cat# NL007). Nuclei were counterstained using DAPI, and cytoplasm using Fluoro Nissl Green (FNG) diluted 1:1 in Northern Lights Guard mounting medium (R&D Systems, Inc., Minneapolis, MN Cat # NL996).

Images were acquired on the Opera Phenix system equipped with a 40x water immersion objective (NA 1.1) and analysed using Harmony software. Three channels representing nuclei, cytoplasm and autophagosomes were acquired simultaneously on a multicamera system in confocal mode. A z-stack of nine planes with $0.5 \mu\text{m}$ distance was acquired from six fields per well. As shown in Figure 2, the morphology and amount of autophagosomes in the untreated cells is quite different between the cell lines. PANC-1 cells appear to have more autophagosomes under control conditions than the other two cell lines. In addition PANC-1 cells are characterized by a higher variation between individual cells in the ground state. While autophagosomes accumulate near the nucleus in HCT 116 cells, PANC-1 autophagosomes seem to be less compact.

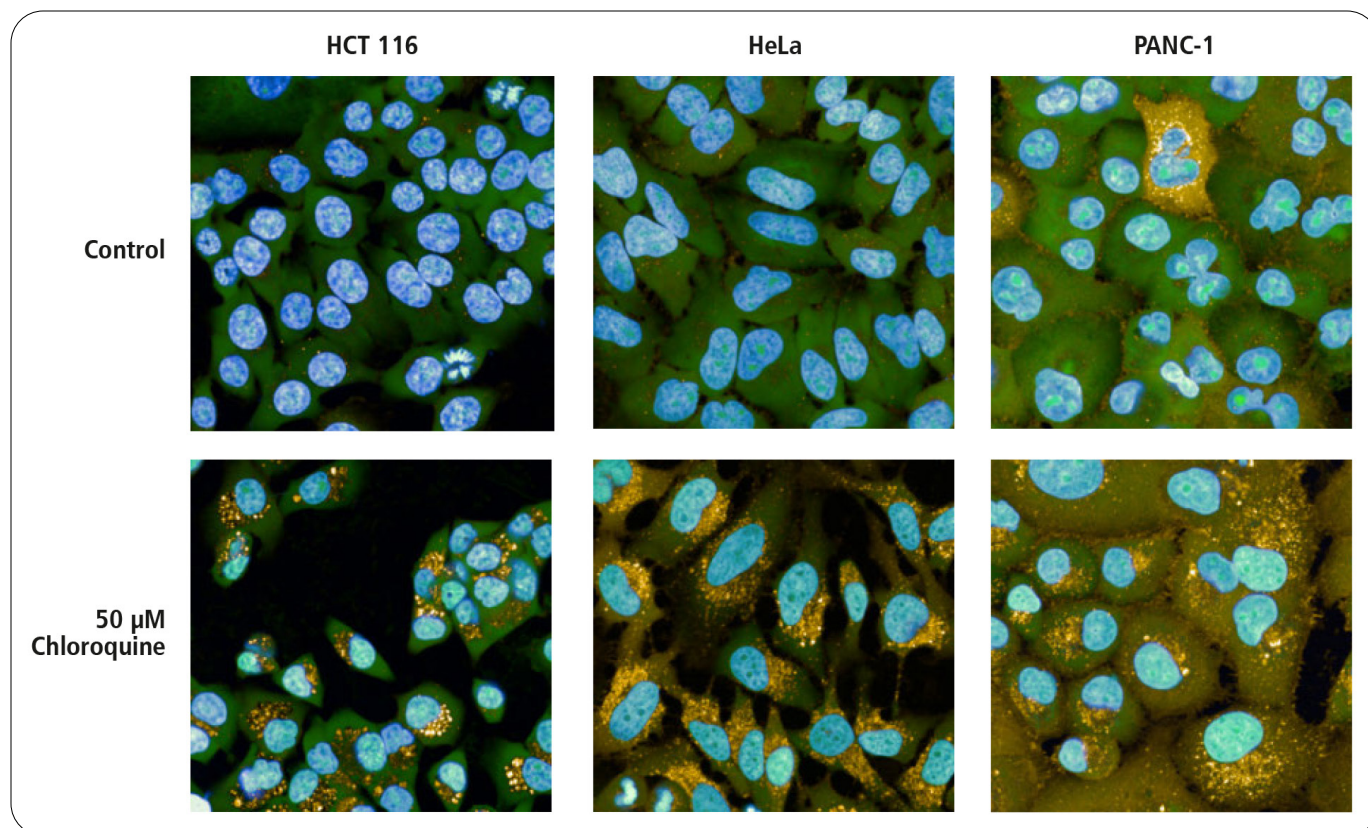


Figure 2: Chloroquine treatment leads to accumulation of autophagosomes in all three cell lines. Chloroquine treated HCT116 (left panel), HeLa (middle panel) and PANC-1 cells (right panel) were stained with SQSTM-1/NL557 (autophagosomes, orange), DAPI (nuclei, blue), FNG (cytoplasm, green) and imaged using a 40x water immersion objective. The number of autophagosomes in untreated control cells (upper panel) was very low and increased after chloroquine treatment (lower panel). The cell line morphology differs in the ground state and cells show individual phenotypic responses to the chloroquine treatment.

Image analysis

The multitude of phenotypic responses (Figure 2) prompted the use of our advanced STAR (Symmetry, Threshold compactness, Axial or Radial) morphology method and SER (Spots, Edges and Ridges) texture analysis. STAR includes a large set of properties and allows the quantification of morphological changes within a certain region. Here, “morphology” refers to the outer shape of objects as well as the distribution of intensities inside the objects. This allows the calculation of several hundred different properties, including among others, parameters describing the symmetric distribution of the staining, compactness parameters describing how densely packed the staining is and profiles which subdivide the cells into different zones such as inner side of plasma membrane (Profile 1/5), cytoplasmic (Profile 2/5), outside of the nuclear membrane (Profile 3/5), inner side of the nuclear membrane (Profile 4/5) and nucleoplasm (Profile 5/5) (see Figure 3 right column).

To allow image analysis, the images were first segmented into nuclei and cytoplasm using the *Find Nuclei* building block on the Hoechst channel and the *Find Cytoplasm* on the FNG channel. To detect autophagosomes the *Find Spots* building block was applied to the SQSTM-1 channel (Figure 3 left column). Then the *Select Population* building block was used to select spots/autophagosomes of certain intensity only.

After image segmentation, a set of basic intensity and morphology properties of the detected autophagosomes was calculated by adding the building blocks *Calculate Intensity Properties* and *Calculate Morphology Properties* (Figure 3 middle column). Furthermore, advanced morphology properties were calculated using the STAR morphology method (Figure 3 right column). Over 300 properties were calculated for each segmented cell to enable classification of two cellular phenotypes (classes): autophagy

positive and autophagy negative cells (Figure 4A and 4B). The PhenoLOGIC supervised machine learning module of Harmony was used, which identifies the properties responsible for the biggest variability in the data from the hundreds reported by the analysis sequence and combines them into a linear classifier to separate the two classes (up to six different classes can be defined)².

The PhenoLOGIC machine learning module is available through the *Select Population* building block. For training, autophagy negative and autophagy positive cells were manually selected. Approximately 100 cells per phenotype are required for training to achieve sufficient sensitivity and specificity. This was done for each of the cell types individually using three separate *Select Population* building blocks.

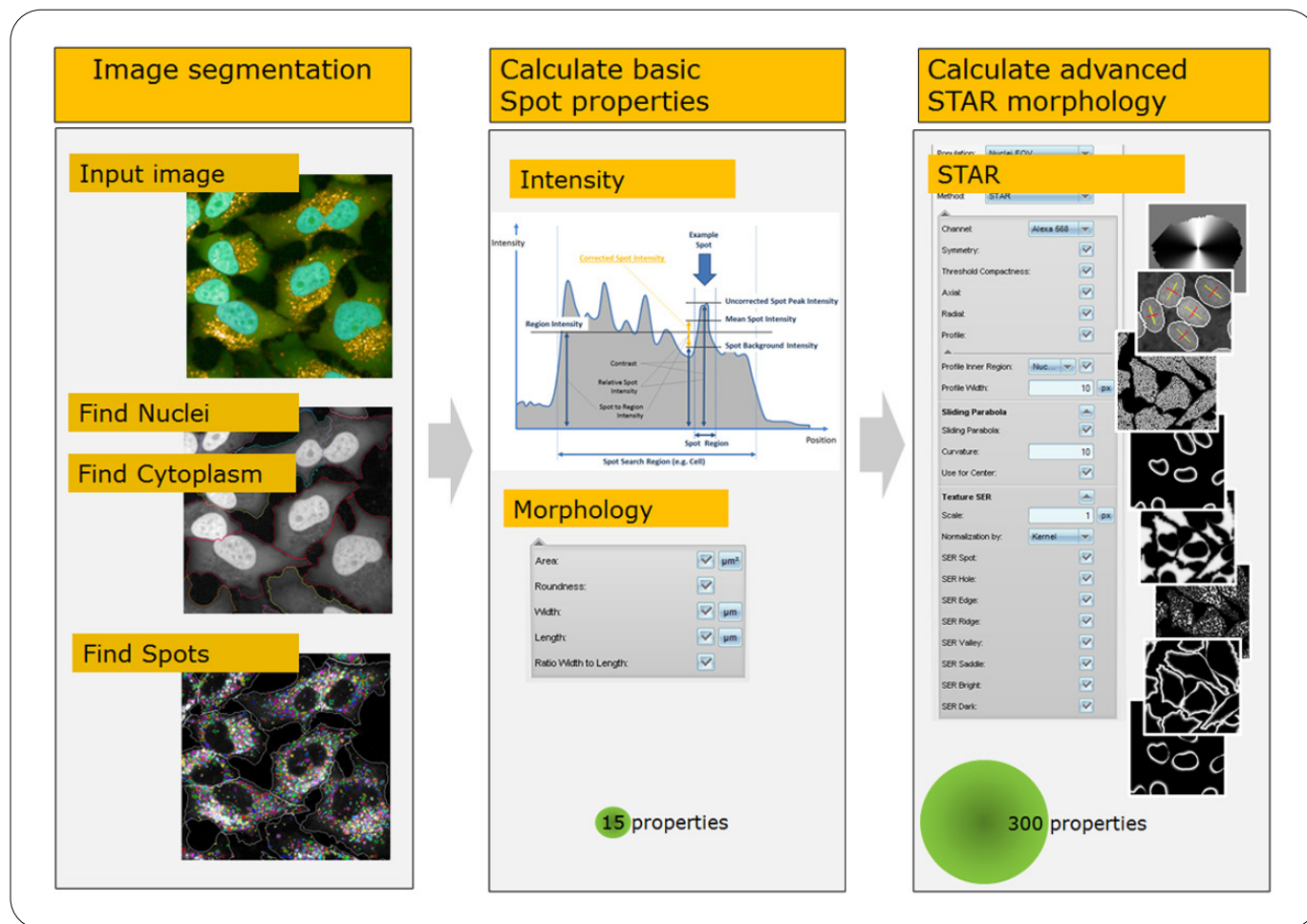


Figure 3: Image analysis workflow from segmentation to STAR morphology (e.g. Cell analysis). Images were segmented into nuclei, cytoplasm and spots using appropriate “Find” building blocks (left panel). Using the building blocks “Calculate Intensity properties” and “Calculate Morphology properties”, basic spot properties were calculated. Using the STAR method, advanced morphology object parameters were determined. In addition to calculating the STAR properties on the original image, several image filters can be selected to pre-process the images before calculating the properties, e.g. sliding parabola or Texture SER. The whole set of STAR morphology properties is then calculated on the filtered images.

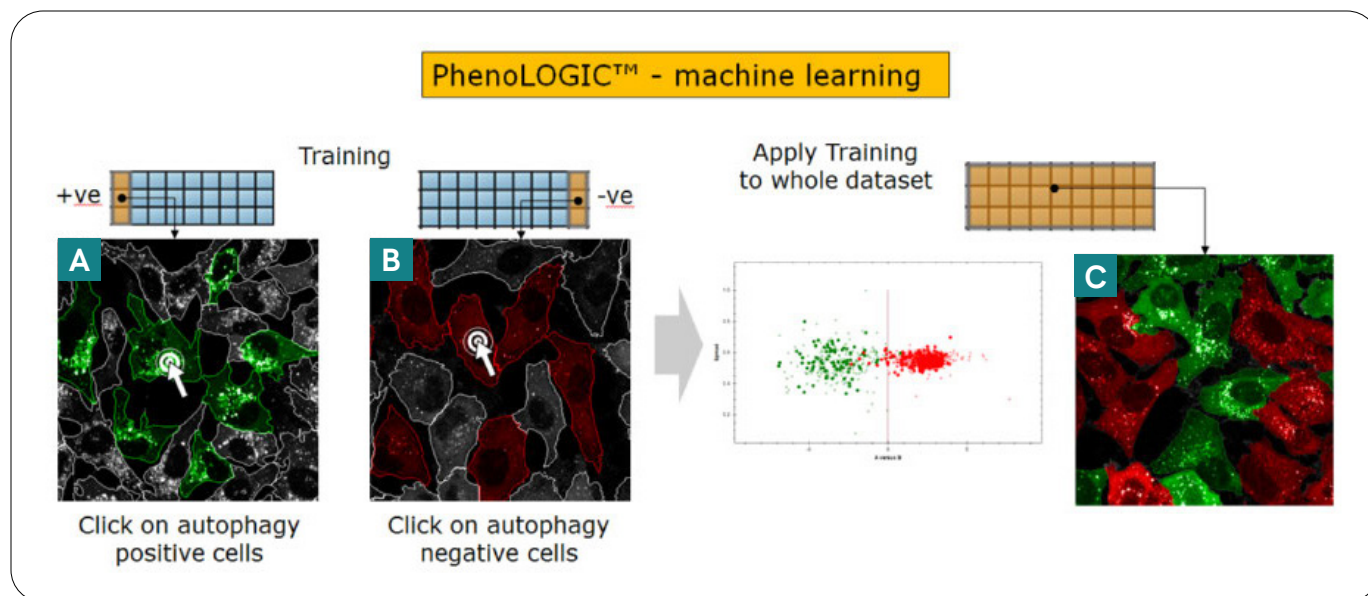


Figure 4: Identifying two cellular phenotypes using the interactive training mode of the PhenoLOGIC machine learning module. In “Training” mode, single cells are manually selected in positive control wells to teach the software to identify autophagy positive cells (panel A, green cells) and autophagy negative cells in negative control wells (panel B, red cells). After training with approximately 100 cells for each class, the classifier can be applied to the whole data set. The software combines the parameters responsible for the biggest variability in the data, whether two, three, four or more, to achieve accurate classification of autophagy positive and negative cells (panel C).

The quantitative image analysis confirmed the visually observed phenotypic changes. Chloroquine treatment led to the accumulation of autophagosomes in all three cell lines. The number and intensity of spots in treated cells increase with increasing chloroquine concentrations (Figure 5 A and B). Also the distribution of spots within the cells changes with increasing chloroquine concentrations indicated by the STAR parameter readouts (Figure 5 D - F). However, none of the calculated Z' values for the different readouts is sufficiently high (> 0.4) to be reliable as a screening assay for all cell lines.

In contrast, the result from the linear classification shows that the newly generated readout, “Autophagy Positive” gives tight EC_{50} curves for all three cell lines and high Z' values indicating

that this is a very robust read out (Figure 6 A). The linear classifier for HeLa cells uses the following spot intensity and STAR properties (ordered by relevance): Relative Spot Intensity, Spots in Cell Profile 2/5 SER-Edge, Cell Profile 2/5, Cell Profile 3/5 SER-Edge, Cell Profile 4/5 SP-Filter, Spots in Cell Profile 1/5 SP-Filter. For the other cell lines, similar relevant properties were extracted by PhenoLOGIC.

To test whether separate training procedures are required for the different cell lines, an additional training in which positive and negative cells were trained equally across all cell lines was performed (Figure 6 B). The results show that the EC_{50} values and Z' values are very similar to the cell line-specific training approach.

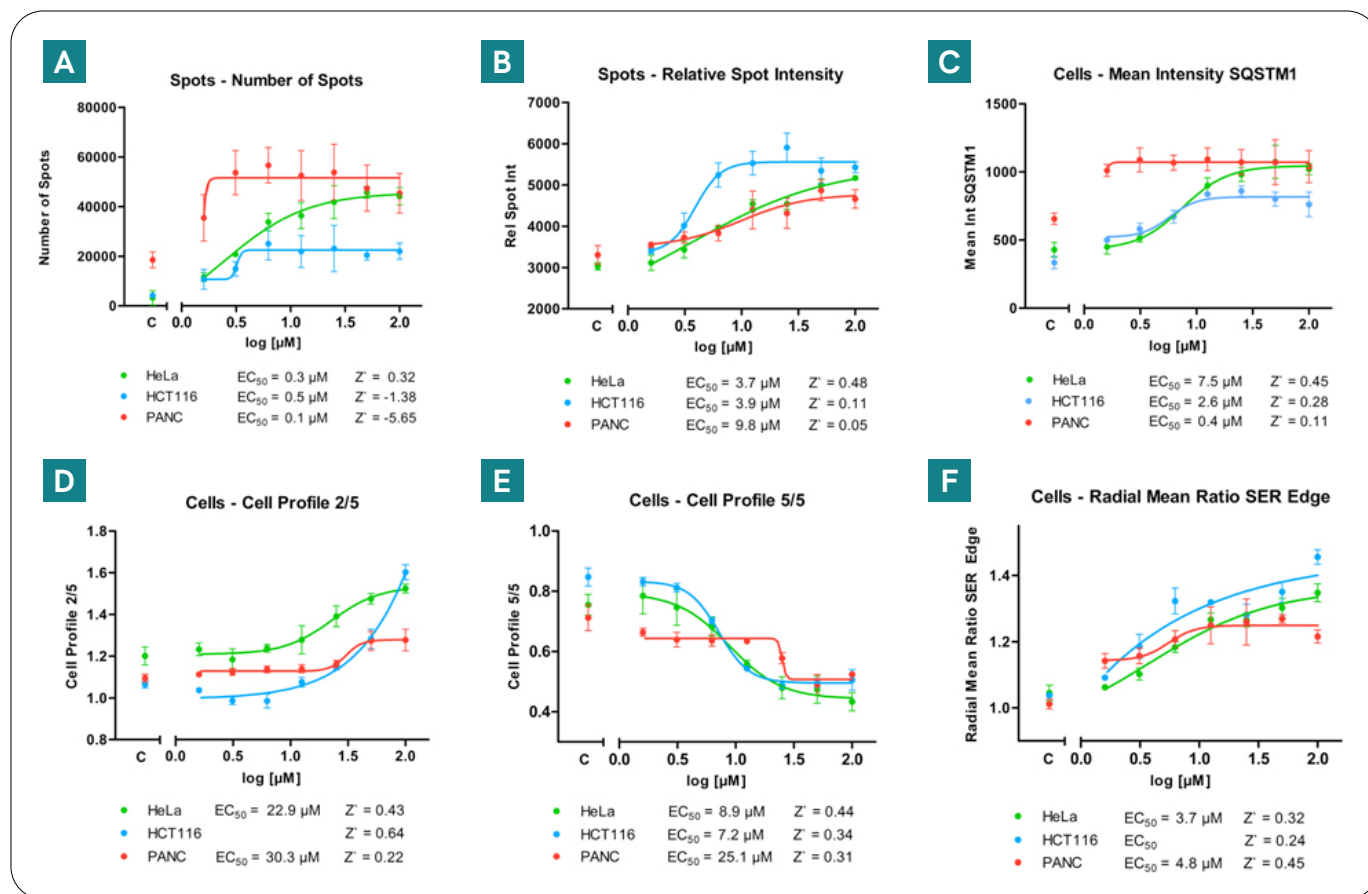


Figure 5: Quantification of chloroquine induced effects on HCT116, HeLa and PANC-1 cells using classical readouts such as spot count and intensity (upper panels) as well as individual STAR morphology readouts (lower panels). Shown are EC₅₀ curves for the different SQSTM1 (autophagosome) readout parameters of both the “Spots” and “Cells” populations. The Z' values indicate that none of them alone is sufficient to describe the changes in all three cell lines. n = 3 wells.

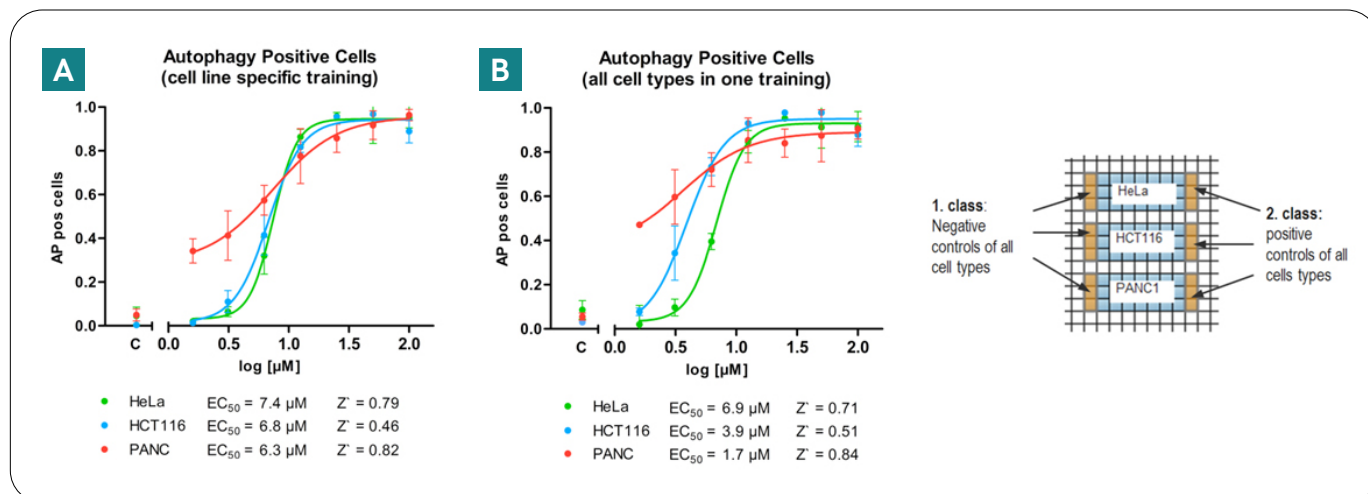


Figure 6: Quantification of chloroquine induced effects on HCT116, HeLa and PANC-1 cells using STAR morphology readouts combined with PhenoLOGIC for classification. Shown are EC₅₀ curves for the readout parameter autophagy positive cells (AP pos cells). The Z' values indicate that this is a robust approach allowing the analysis of the cells either using separate training blocks for each cell line (A) or using one training block for all three cell types (B). For the latter, positive and negative cells were equally trained across the three cell lines. n = 3 wells.

While Harmony and the PhenoLOGIC linear classifier are efficient tools for small scale experiments during assay development or for analysis of a small number of plates, Harmony is less well suited to handling large amounts of screening data. For this task our secondary analysis software High Content Profiler™ is built on TIBCO Spotfire®. High Content Profiler provides an automated way to handle large data sets. While it generates comprehensive data visualizations to better understand the screening data, it also greatly supports phenotypic screening approaches by processing hundreds of readouts and providing unsupervised and semi-supervised machine learning tools for cell classification.

Secondary data analysis in high content profiler

To demonstrate the power of this secondary analysis tool, the multiparametric autophagy dataset was imported into High Content Profiler (HCP). HCP automatically guides the user through a series of steps providing Normalization, Quality Control, Feature Selection and Hit Stratification. In this application, the cell-level and well-level data resulting from the image analysis completed in Harmony was analyzed. First quality control and data clean-up on the cell level data was performed, by utilizing trellised scatter plots and direct image rendering to identify and remove outliers (Figure 7). The standard deviation of triplicates within each cell line was significantly lower with cell-level data QC, compared to using aggregate well-level values that included all cell-level values. For this reason alone, capturing cell level data and performing QC before aggregating it to well-level can greatly improve the accuracy of analysis.

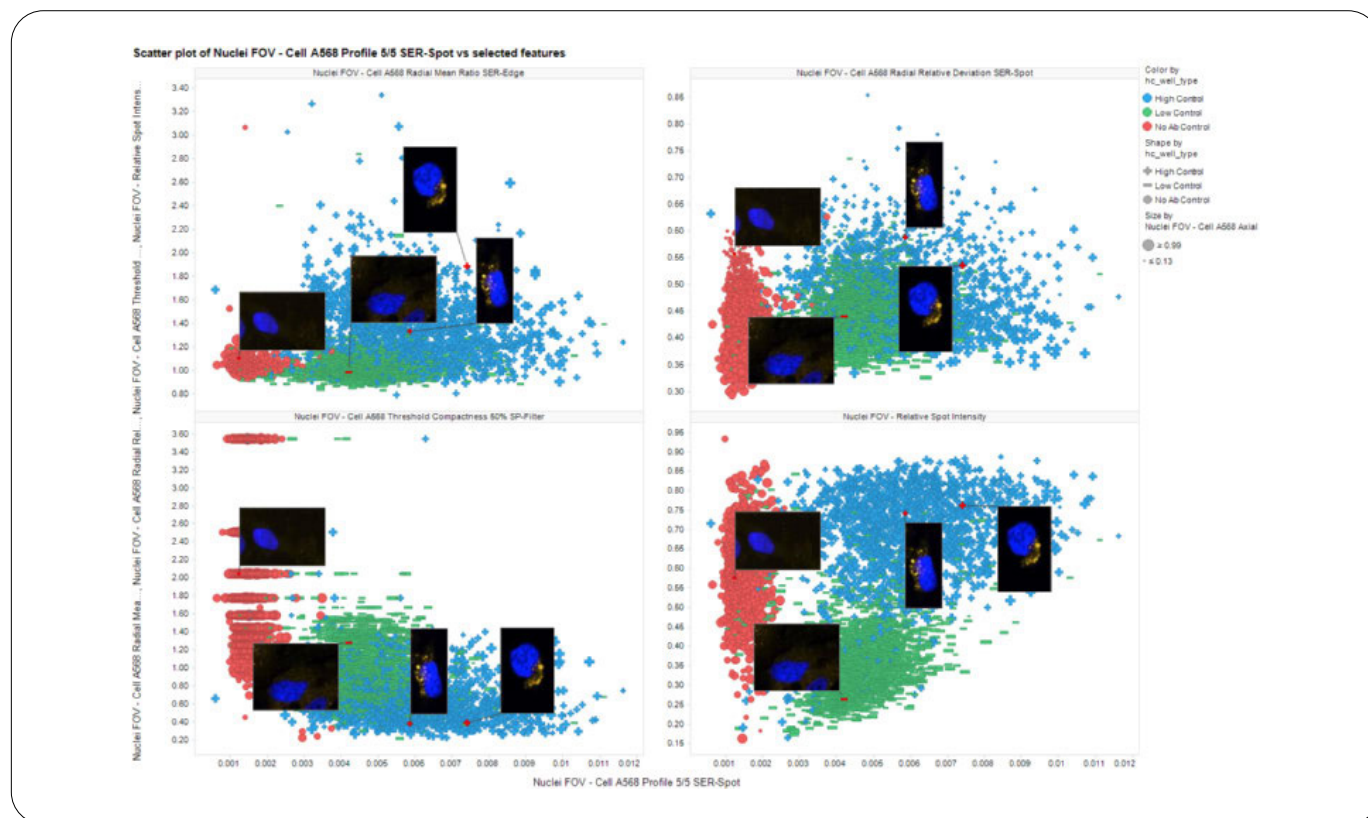


Figure 7: An array of scatter plots enables the visualization of sub-populations, separation of treatment groups and identification of potential outliers, which can then be removed from the analysis. For instance, cells that did not express any autophagosome signal, similar to the unlabeled controls highlighted in red. Representative cell images are displayed for validation.

Analyzing the cell-level data allowed the exploration of the heterogeneity of responses across the three cell lines and the identification and selection of subpopulations or unique

phenotypes. High Content Profiler provides box plot and histogram visualizations to help understand the level of heterogeneity and presence of subpopulations (Figure 8).

It is readily apparent that the dose response of chloroquine across the three cell lines varies, as well as the distribution of autophagosome positive cells. In this view, many of the calculated parameters from the image analysis were explored and a deeper examination of the parameters put forth by Harmony was performed.

Following cell-level QC and analysis, results were aggregated to well level for further analysis including machine learning for profiling and comparison to PhenoLOGIC results. High Content Profiler provides both semi-supervised and unsupervised machine learning techniques to discover clusters, trends, batches and outliers. Autophagosome classification from PhenoLOGIC was only used for comparison purposes and was not included in the HCP analysis. First Principal Component Analysis³ utilizing all calculated parameters was explored and dose-dependent effects of chloroquine across all three cell lines were clearly seen. More interestingly, the phenotypic response of all three cell lines clustered separately on PCA, even the untreated

cells (Figure 9). The data can be inspected in another way utilizing an unsupervised machine learning technique called Self-Organizing Map algorithm⁴. It is a type of artificial neural network that clusters similar profiled data points together, in this case the aggregate phenotypic profile of each well of our assay. If two data points have extremely similar profiles, they will be clustered together in the same node. The Sammon Connection Networks plot is used to visualize the results of the SOM in a two-dimensional way. The farther away two nodes are, the more dissimilar to each other and the length of the line connecting two nodes also indicates how similar or dissimilar. It was found that the three cell lines had very different profiles from each other and the low, medium and high doses of chloroquine also gave distinct profiles (Figure 10). All wells designated as a 'No antibody control' clustered together in the center of the plot. This shows that the phenotypic response to chloroquine is indeed very different in the three cell lines, which was almost indistinguishable by eye. These results also coincide with the finding from the PCA in Figure 9.

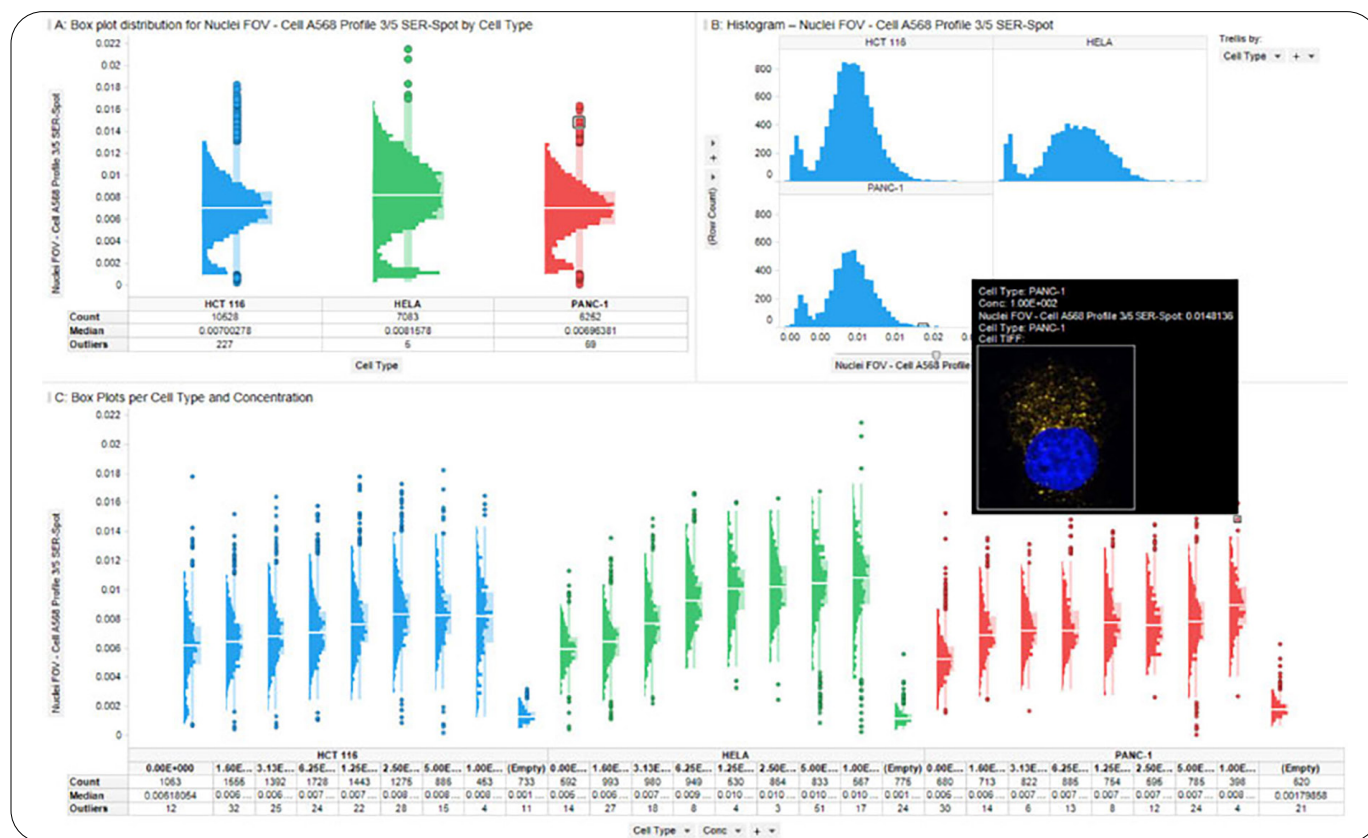


Figure 8: Box plots and histograms allow the visualization of statistical measures of a chosen parameter as well as the distribution of that parameter. These visualizations also work well to indicate potential outliers which can then be confirmed with images and removed from the analysis. A and C: Box plots showing the distribution of data points across cell types and cell types with concentrations, respectively. The parameter of interest is the spot texture profile in the cell region just outside the nuclear membrane. The white line indicates the median value and the data points outside of the first and third quartiles are displayed as outliers. B: Histogram of the same parameter across cell lines show bimodal distribution. Potential outlier cell image is displayed for validation.

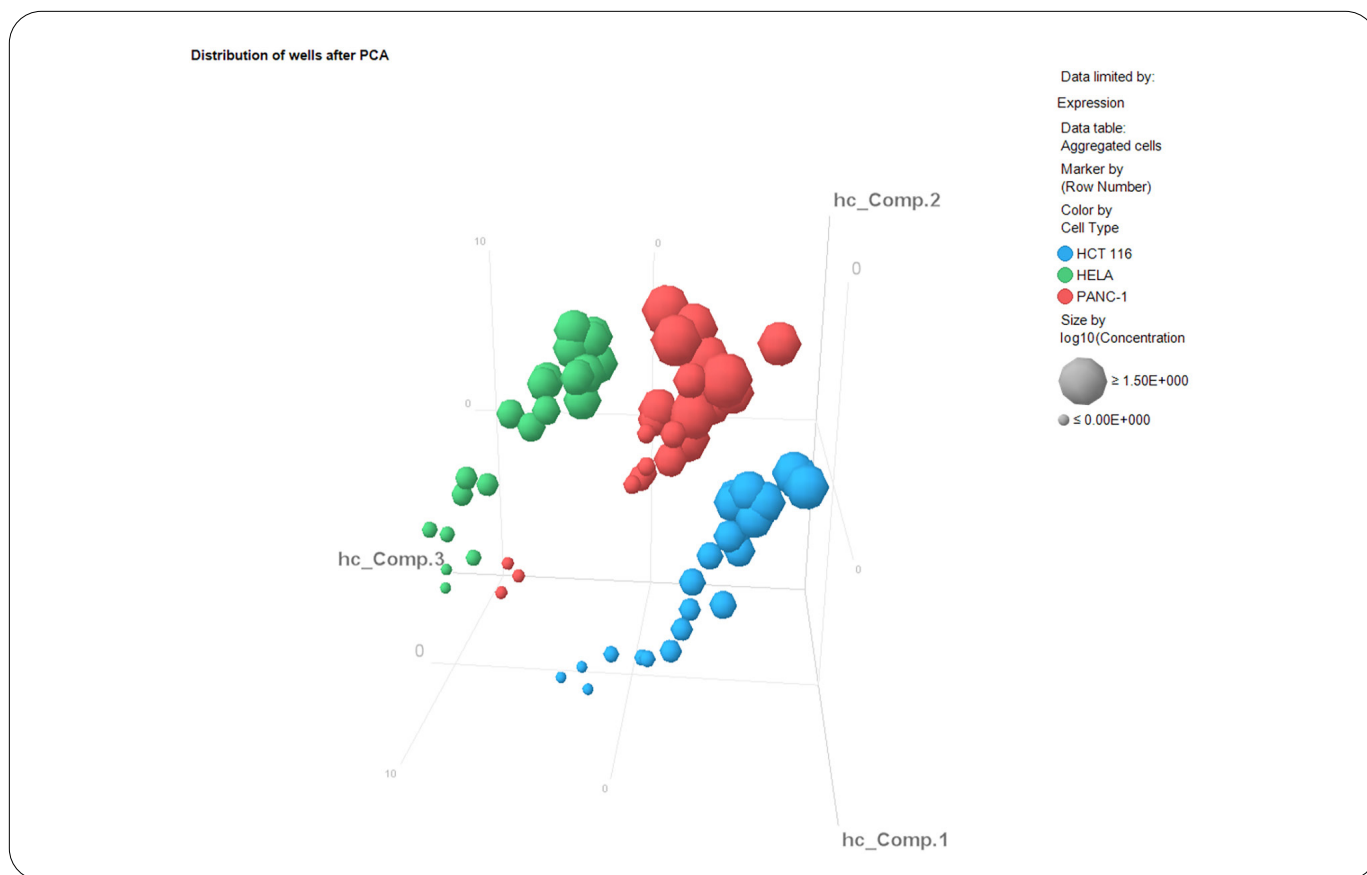


Figure 9: Principal Component Analysis (PCA) visualization of all cell lines and concentrations of chloroquine. HCT116 seeded wells are represented by blue spheres, HeLa by green and PANC-1 by red. The concentrations of chloroquine are represented by the size of the spheres (larger spheres represent higher concentrations).

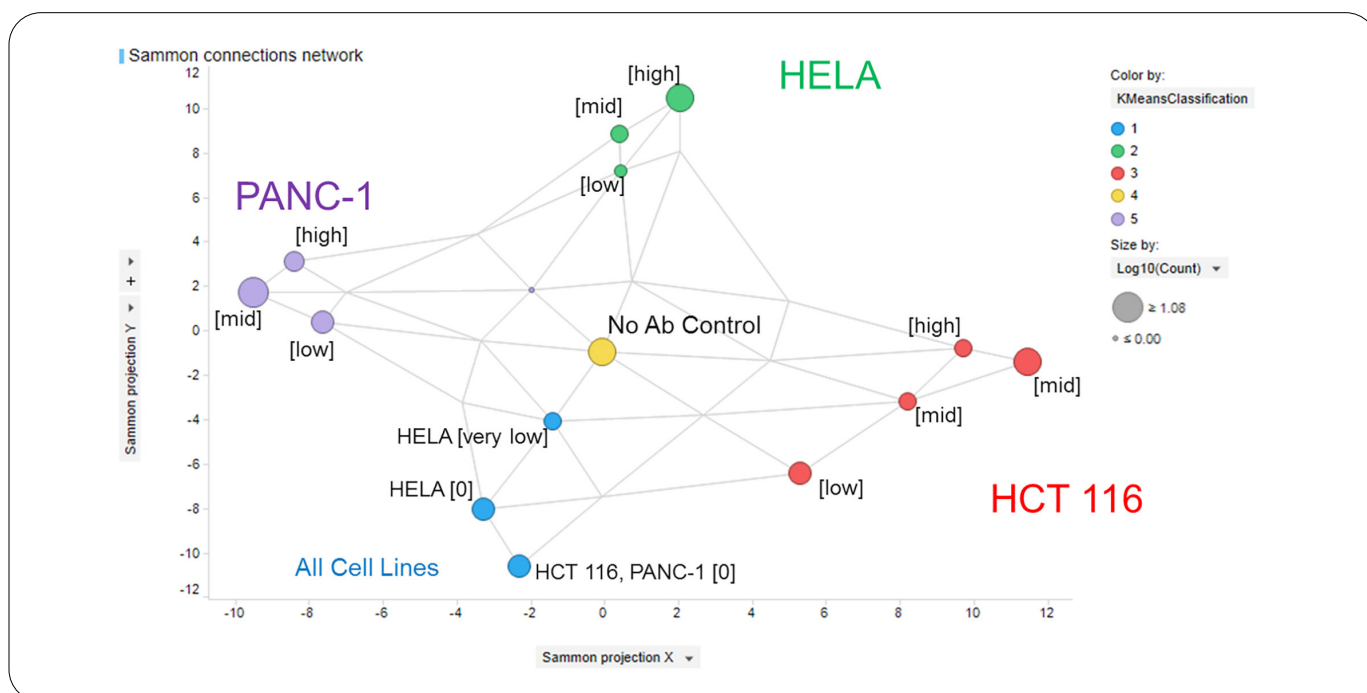


Figure 10: Self-Organizing Map and Sammon Connection Network clearly separate and cluster the three different cell lines as well as the different concentrations of chloroquine based on all the features extracted from image analysis. Each circle represents a node identified by SOM. The nodes are colored by the K-means clustering algorithm and the input was five clusters.

Lastly, semi-supervised machine learning methods were used to perform Feature Selection and Hit Classification. The machine learning is semi-supervised because positive and negative control designations are inputs generated by the scientist. The algorithms chosen for this particular application were Ensemble Based Tree Classifier (Random Forest)⁵ for both feature selection and hit classification. While the PhenoLOGIC machine learning uses a linear algorithm, the Random Forest algorithm builds classification trees to look at the best combination of parameters to find the most relevant in describing the variance between two end points. While not an exact one-to-one match was made between the two methods, similar parameters rose to the top: Cell Profiles of the autophagosome staining as well as its Threshold Compactness. These are calculated from the STAR Morphology analysis building block. High Content Profiler then reduces the number of parameters to just the most relevant ones and performs hit stratification and classification, thus identifying which wells are 'autophagosome positive' versus 'autophagosome negative'. Dose response curves (DRCs) are automatically generated if the treatment is titrated, as in this example (Figure 11). DRCs can be viewed for individual parameters, as in Harmony, and the different EC₅₀ values for each cell line

can be seen. It can also be compared to a parameter called "Positivity Score" which is a multivariate, phenotypic score based on the relevant parameters drawn out by the semi-supervised machine learning. A curve based on this parameter will be more robust than that of any single parameter, similar to the autophagy positive readout generated by the linear classifier in Harmony.

The classification result obtained by semi-supervised classification in HCP (Figure 11) coincides very well with the result obtained by supervised machine learning in Harmony (Figure 6). The PANC-1 cell curve is distinct from the other two cell lines, while HCT 116 and HeLa cells show similar curves, although HeLa cells score slightly higher than HCT 116 cells when classified with HCP. As expected, the EC₅₀ values for HeLa and HCT 166 cells based on the positivity score DRC are similar (HeLa = 7.9 μM and HCT 116 = 7.8 μM) and within the same range as EC₅₀ values obtained by the Linear Classifier in Harmony (HeLa = 7.4 μM and HCT 116 = 6.8 μM), while no EC₅₀ value can be inferred from the PANC-1 curve. Therefore it can be concluded that both Harmony and HCP are able to classify the two phenotypes autophagy positive and autophagy negative alike.

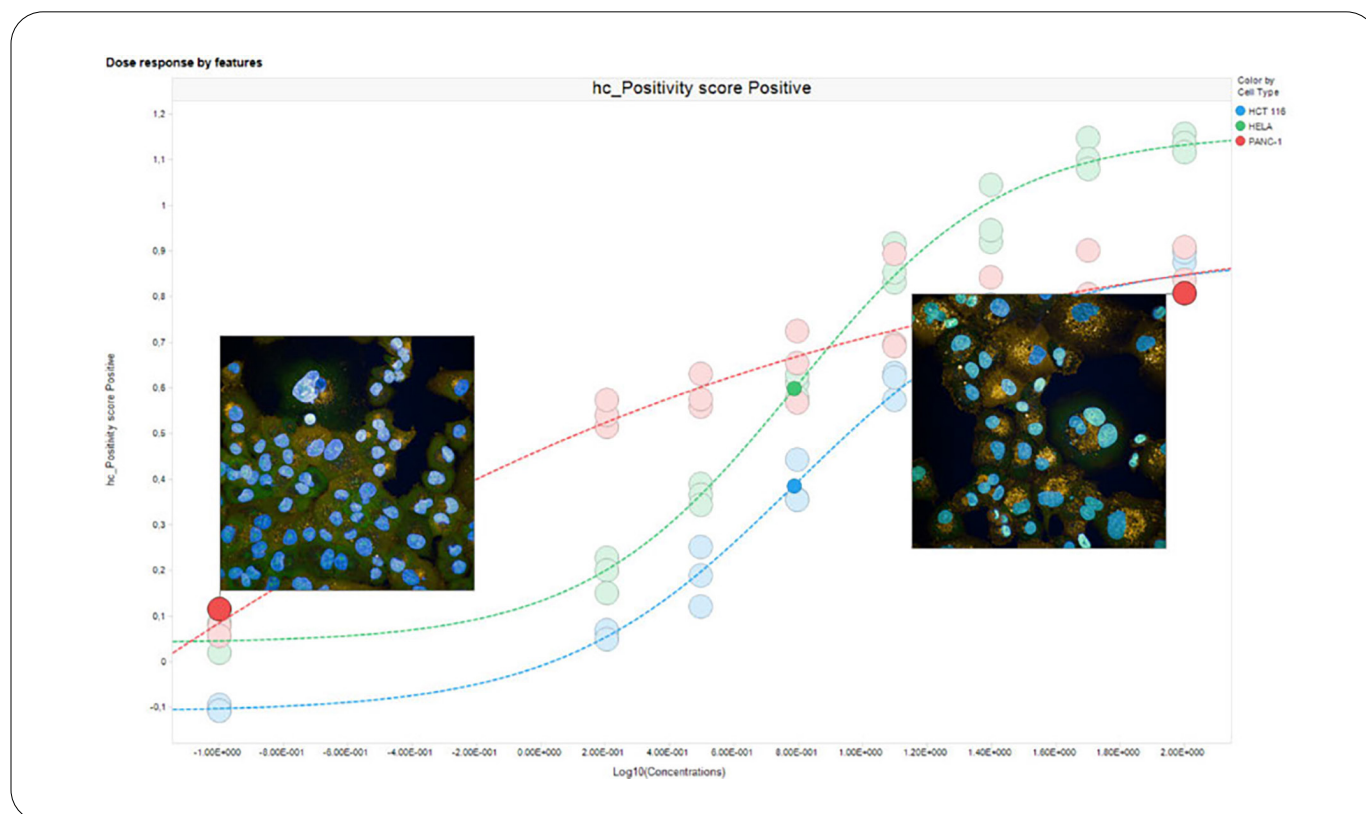


Figure 11: Dose response curves of all three cell lines in HCP. A multivariate score called "Positivity Score" is used as the measure on the y-axis. Representative images at points across the curve are displayed for validation.

Conclusions

Image processing, statistical analysis of multiparametric data, and phenotypic profiling at both individual cell and aggregated well level are increasingly becoming a bottleneck in HCS analysis. In this study, we validate a phenotypic image and data analysis workflow provided by Revvity's Harmony and High Content Profiler software using an autophagy assay as an example application.

Harmony is ideally suited for image analysis of phenotypic assays. With its advanced morphology readout toolkit including Texture and STAR analysis, Harmony is able to calculate hundreds of phenotypic readouts per cell. Machine learning techniques like the Linear Classifier then help to identify the most relevant readouts and allow readouts to be combined to better discriminate phenotypes whenever a single readout is not sufficient. Therefore it is easy for the biologist to analyze rich phenotypic data, by simply pointing and clicking on the cells in the image, telling the software which classes they belong to.

However, Harmony's significant strength for phenotypic screening becomes apparent when combined with secondary analysis tools such as High Content Profiler. Harmony and High Content Profiler work seamlessly together and HCP provides a much more automated way of handling large data sets. It creates a set of standardized reports that help assess and improve the quality of the screening data as well as identifying the most relevant readouts and classifying the cells using unsupervised and semi-supervised machine learning algorithms.

Finally, if the treatment is titrated, EC_{50} curves are automatically generated. All of these tools should ultimately facilitate the decision whether to proceed with a certain compound, particular gene or molecular target.

For the autophagy assay described here, both supervised machine learning in Harmony and semi-supervised machine learning in HCP lead to similar EC_{50} curves (compare Figures 6 and 11), probably because of a relatively simple phenotypic change in all three cell lines. However, both supervised machine learning, and unsupervised classification tools such as principal component analysis or self-organizing maps, are great tools within their own rights. While the supervised linear classifier is helpful whenever the phenotypes are predicted by the user, unsupervised classification might be better suited for applications with an unknown number of phenotypes. It might also detect subtle phenotypic changes that the user had not seen by visual inspection of the images. However, unsupervised methods might sometimes lead to classifications based on side effects such as slightly different cell densities or exposure settings during imaging, rather than the biological effect the user is seeking. In these cases biological knowledge can help steer the machine learning process.

Taken together, Harmony and High Content Profiler provide a breadth of tools to analyze, classify and interpret phenotypic screening data, which ultimately helps to make better decisions faster.

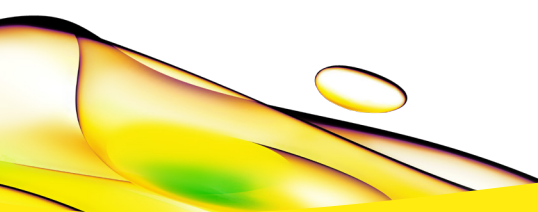
References

1. Choi, A. M. K., Ryter, S. W., & Levine, B. (2013). Autophagy in human health and disease. *N Engl J Med*, 368(19), 1845-1846. doi:10.1056/NEJMc1303158
2. Fisher, R. A. (1936). The Use Of Multiple Measurements In Taxonomic Problems. *Annals of Eugenics*, 7(2), 179-188. doi:10.1111/j.1469-1809.1936.tb02137.x
3. Pearson, K. (1901). LIII. On lines and planes of closest fit to systems of points in space. *Philosophical Magazine Series 6*, 2(11), 559-572. doi:10.1080/14786440109462720
4. Kohonen, T. (1982). Self-organized formation of topologically correct feature maps. *Biological Cybernetics*, 43(1), 59-69. doi:10.1007/BF00337288
5. Breiman, L. (2001). Random Forests. *Machine Learning*, 45(1), 5-32. doi:10.1023/A:1010933404324

Authors

Stefan Letzsch
Michelle Walk
Seungtaek Lee
Alexander Schreiner
Karin Boettcher
Revvity, Inc. Hamburg, Germany

Alex Kalyuzhny
Jodi Hagen
R&D Systems, Minneapolis, USA



revvity